• 物理电子学 •

Research on Terahertz Backward-Wave Oscillator Based on Photonic Column Array Slow-Wave Structure

XIAO Chuanhong[1], WU Zhenhua[1*], LI Jielong[1], SHI Zongjun[1], ZHONG Renbin[1], LIU Diwei[1], ZHAO Tao[1,2], HU Min[1], and LIU Shenggang[1]

(1. School of Electronic Science and Engineering, University of Electronic Science and Technology of China Chengdu 611731;
2. Higher Research Institute (Shenzhen) of University of Electronic Science and Technology of China Shenzhen Guangdong 518110)

Abstract This article explores a photonic column array slow-wave structure (SWS). A 0.28-THz sheet beam backward-wave oscillator (BWO) was designed and simulated by calculating the dispersion, field distribution and particle simulation. When the cathode current density is only 10 A/cm^2 (the minimum is less than 6 A/cm^2), the voltage is 12.5 kV and the magnetic field is 0.5 T, the structure interacts with the sheet beam by immersion and the output power is 435 mW. On the basis of previous work, the SWS was fabricated using Lithography-Galvanoformung-Abformung (LIGA) fabrication technology. The results show that the column array structure can effectively improve the interaction efficiency and reduce the starting current density; and effectively improve the lifespan of terahertz (THz) vacuum electron device (VED) cathodes, which is a viable means of increasing the performance of THz vacuum radiation sources.

Key words column array slow-wave structure; THz BWO; starting current; vacuum electron device

基于光子晶体慢波结构的太赫兹返波管研究

肖川红[1]，吴振华[1*]，李杰龙[1]，史宗君[1]，钟任斌[1]，刘頔威[1]，赵 陶[1,2]，胡 旻[1]，刘盛纲[1]

(1. 电子科技大学电子科学与工程学院 成都 611731；2. 电子科技大学 (深圳) 高等研究院 广东 深圳 518110)

【摘要】研究了一种光子晶体的慢波结构，通过对该结构的色散、场分布和粒子模拟计算，设计和仿真了一个 0.28-THz 的带状注返波管。在阴极电流密度仅 10 A/cm^2(最小可低于 6 A/cm^2)，电压 12.5 kV，磁场 0.5 T 的情况下，该结构通过与带状电子注浸没式互作用，输出功率为 435 mW。在此基础上，采用了 LIGA 加工技术制备了该慢波结构。研究表明，光子晶体结构能有效提高互作用效率和降低起振电流密度，有效提高太赫兹真空电子器件阴极的使用寿命，是提高太赫兹真空辐射源性能的一种有效途径。

关 键 词 光子晶体慢波结构； 太赫兹返波管； 起振电流； 真空电子器件
中图分类号 TN12; O46 **文献标志码** A doi:10.12178/1001-0548.2022014

The interest in millimeter and terahertz (THz) waves is on the rise due to their unique properties and suitability for a wide range of applications[1-3]. Thanks to advancements in the microfabrication technology, high-powered vacuum electron devices (VEDs) are capable of generating microwaves in the millimeter and THz range[4-5].

In a typical VED, the amplitude of the

Received date: 2022 − 01 − 07; Revised date: 2022 − 05 − 27
收稿日期：2022 − 01 − 07；修回日期：2022 − 05 − 27
Foundation item: Supported by National Natural Science Foundation of China (61701084, 61505022); National Key Research and Development Program of China (2018YFF01013001, 2017YFA0701000)
基金项目：国家自然科学基金 (61701084, 61505022)；国家重点基础研究专项 (2018YFF01013001, 2017YFA0701000)
Biography: XIAO Chuanhong was born in 1992, male, PhD, his research interests include vacuum electron device.
作者简介：肖川红 (1992 −)，男，博士，主要从事真空电子器件等方面的研究.
*Corresponding author: WU Zhenhua, E-mail: wuzhenhua@uestc.edu.cn
*通信作者：吴振华，E-mail：wuzhenhua@uestc.edu.cn

synchronous slow-wave z-component in the electric field (E_Z) decreases as its distance from the structure increases. Only a thin layer of electrons moving close to the structure can effectively interact with this high-frequency E_Z field. At the millimeter- and terahertz-wave band, the beam interacting with the high-frequency E_Z field decreases. A number of methods have been proposed to improve VEDs, through increasing efficiency and decreasing starting current density[6-8]. There have been attempts at using sheet electron beam devices[9-11] to improve VED performance by enlarging interaction space and providing sufficiently high currents. High-operating current density reduces the lifespan of cathodes in millimeter-wave and THz VEDs, therefore, currents should be kept as low as possible.

This article explores the photonic column array slow-wave structure (SWS), in order to improve the performance of THz VEDs[12-18]. The study designed and simulated a 0.28-THz backward-wave oscillator (BWO). The photonic column array SWS allows the flow of sheet beams. A planar SWS is a multi-column structure, which collects a large number of electrons on the surface of its columns. More electrons are lost in column array structures than in comb structures. This allows for the reduction of the starting current density in multi-column structures through increasing the length or width of the structure. Higher operating voltages (10～20 kV) can then be used to provide significant power and frequency increases. This article focuses on the design and analysis of a 0.28-THz BWO. We show that photonic column array structures are effective in improving the operation of microwave VEDs, such as BWOs.

1 Model of the photonic column array SWS

A schematic of the photonic column array SWS is shown in Fig. 1. The periodic slot-hole structure in this model can be extended along its length or breadth. Electron beams may flow through the structure, which increases the effective interaction of current with the slow-wave field. This makes the structure promising for applications in THz VEDs.

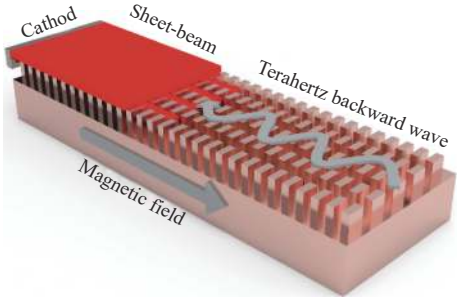

Fig. 1　The photonic column array SWS

The parameters of the structure are shown in Fig. 2. To enable a VED operating at 0.28 THz, the dimensions of the structure were chosen as follows: d_1 = 0.17 mm, a_1 = 0.08 mm, d_2 = 0.30 mm, a_2 = 0.12 mm, and h = 0.20 mm. Fig. 2b shows the E_Z field amplitude as a function of distance at a frequency of 0.28 THz. The E_Z field peaked at height h=0.20 mm. The beam interacted with the E_Z field inside the structure, so it can be seen from Fig. 2b that the beam thickness is δ = 0.30 mm. This increased the effective beam-wave interaction.

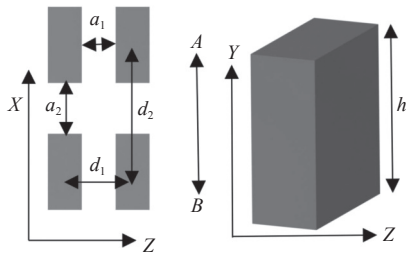

a. Dimensions of the SWS

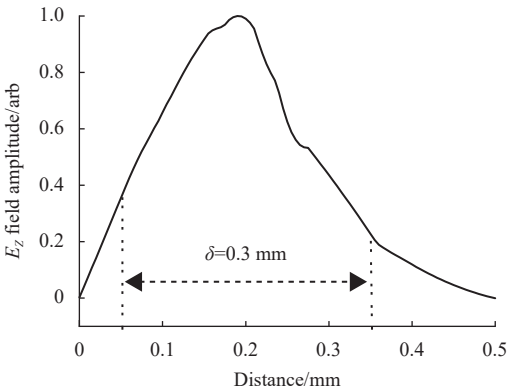

b. EZ field amplitude as a function of distance (line AB in Fig. 2a)

Fig. 2　Dimensions of the photonic column array SWS and electric field amplitude at gap

The simulation software CST was used to analyze the cold cavity. After the simulation calculation, the dispersion curves of the photonic column array SWS,

for BWOs are shown in Fig.3. The point of beam-wave interaction (at about f = 280 GHz) and the intersection of the dispersion curve with the beam lines for 10 kV, 12.5 kV and 15 kV electrons are shown in Fig. 3. The operating frequency is changed by adjusting the operating voltage. The electric field distribution of the TM_{11} mode is shown in Fig. 4.

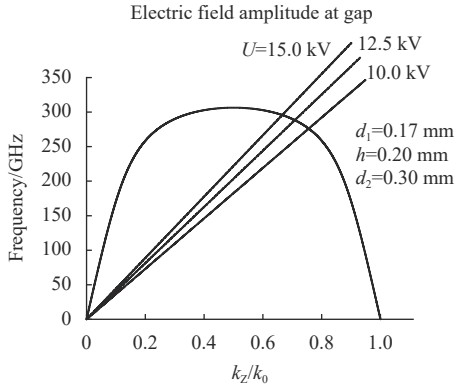

Fig. 3 Dispersion curves of the photonic column array SWS

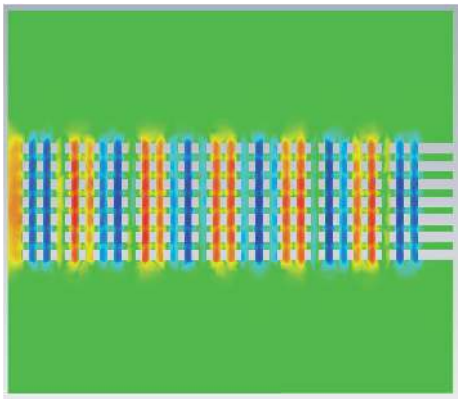

a. EZ field distribution on the X–Z plane

b. EZ field distribution on the Y–Z plane

Fig. 4 Field distribution of the TM_{11} mode in the photonic column array SWS

2 Design and simulation of a 0.28-THz BWO

A 0.28-THz BWO was designed and simulated using CHIPIC, a three-dimensional (3D) electromagnetic particle-in-cell (PIC) finite-difference time-domain (FDTD) code. The system used the photonic column array SWS.

The SWS and baseplate cover consisted of copper. The simulation parameters of the BWO are shown in Table 1. Fig. 5 shows the electron beam passing through the photonic column array SWS on the Y-Z and X-Z planes. The THz signal output through a coupler, which consisted of a slot coupled to a WR10 waveguide.

Table 1 Operating parameters of the BWO

Parameters	Value
Beam voltage/kV	U = 12.5
Beam current/mA	I = 78
Beam thickness/mm	δ = 0.3
Current density/A·cm^{-2}	10
Number of periods	N = 80
External magnetic field/T	0.5
Baseplate-cover height/mm	H = 0.45

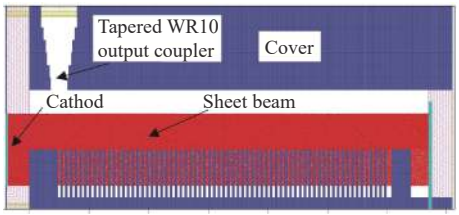

a. The electron beam passing through the SWS at the Y–Z plane

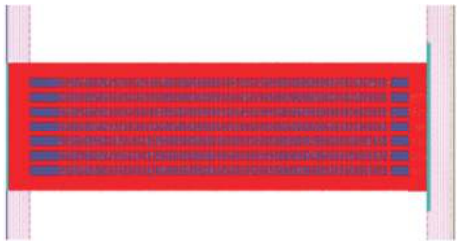

b. The electron beam passing through the SWS at the X–Z plane

Fig. 5 Position distribution of the electron beam in the SWS

The results of the PIC simulation are shown in Fig. 6. The average beam energy was reduced through absorption by the SWS, as shown in Fig. 6a. The total current in the SWS was 78 mA, and the interaction current was about 51.5 mA. About 29.7% of electrons were lost in the multi-column structures, because the sheet beam was immersed in the SWS, as shown in Fig. 5a. However, this increased the surface of the beam-wave interaction.

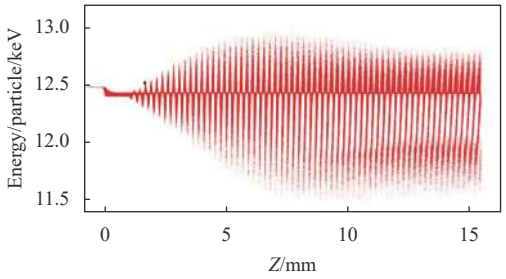

a. Electron energy as a function of SWS length

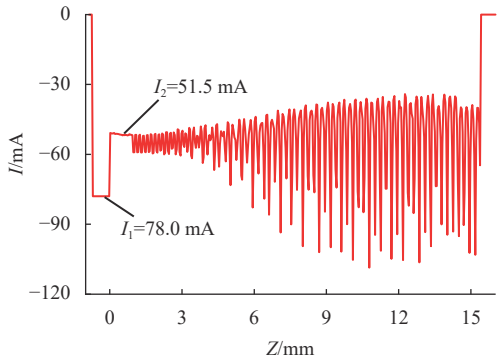

b. Electron current as a function of SWS length

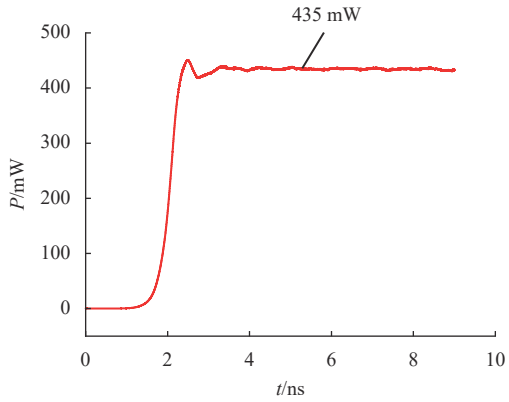

c. Output power

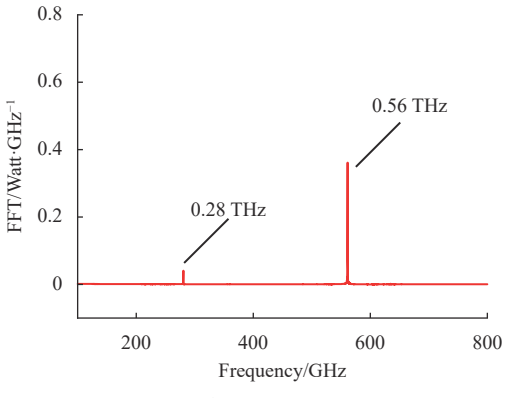

d. Power spectrum

Fig. 6　The results of PIC simulation

The output power as a function of time, and the corresponding FFT power spectrum are shown in Figs. 6c and 6d, respectively. In accordance with the power law $P \propto E^2$, the amplitude on the FFT power spectrum corresponding to 0.56 THz was much higher than that corresponding to 0.28 THz. The operating frequency of 0.28 THz matches the intersection in Fig. 3.

Fig. 7a shows the high-frequency field power as a function of SWS length. Most of the field power was retained in the BWO, unlike the output power in Fig. 6c. This shows that the output coupling efficiency of this device was very low. Fig. 7b shows the surface power loss in the BWO. Surface power loss was much higher than the output power loss shown in Fig. 6c. Power loss to structures cannot be ignored in simulations, especially for high-frequency devices.

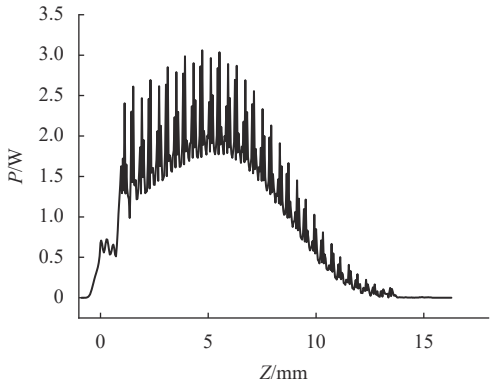

a. Field power as a function of SWS length

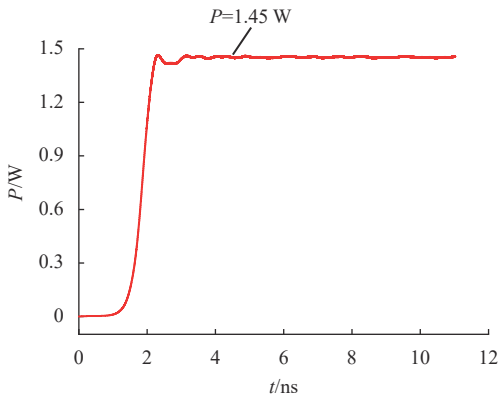

b. Surface power

Fig. 7　High-Frequency field power and loss

Fig. 8 shows power as a function of various parameters. Fig. 8a shows that the power increased as the number of periods increased, and Fig. 8b shows that power increased as the number of rows increased. After a series of calculations and comparisons, the numbers of periods and rows were chosen to be 80 and 7, respectively.

Sweeping simulation of the beam voltage, as

shown in Fig. 8c, shows that the power peaked at operating voltage U = 12.5 kV, and the frequency increased with increasing voltage. This suggests that the operating frequency of the oscillator can be changed by adjusting the operating voltage. Power increases with increasing current density, as shown in Fig. 8d. The BWO functioned at a current density of 6 A/cm^2 and must maintain a relatively low operating current density to increase the lifespan of the cathode. Referring to Fig. 8e, the output power increased as the guiding magnetic field increased. Stronger magnetic fields increased the size and cost of the device. A 0.5-T guiding magnetic field was adopted for the device in this study.

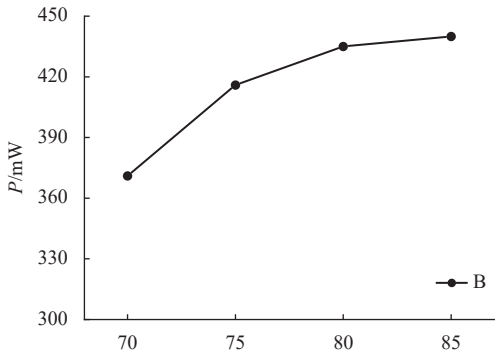

a. The number of periods in the SWS

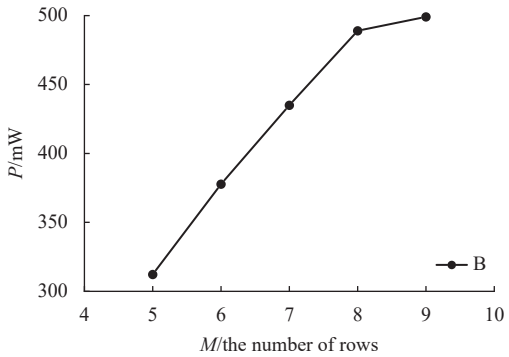

b. The number of rows in the SWS

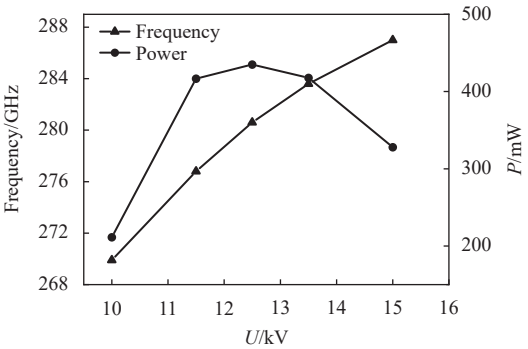

c. Power and frequency as a function of beam voltage

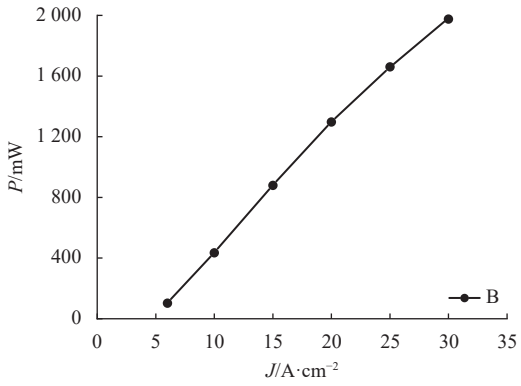

d. Current density

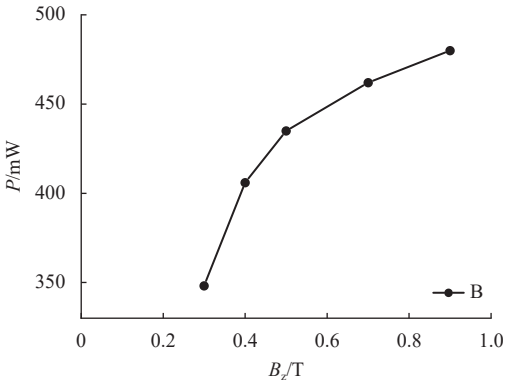

e. Axial magnetic field

Fig. 8 Output power as a function of different parameters

3 Fabrication

The structure was fabricated using the lithography-galvanoformung-abformung (LIGA) fabrication technology, as shown in Fig. 9. Some issues were identified using a scanning electron microscope (SEM), manufactured by ZEISS. First, thin irregular burrs were found on the top of the structure, as highlighted by the blue squares in Fig. 9. These burrs were formed during the polishing process, and they may obstruct beam-wave interaction. The burrs can be removed with applied acid or thermal shocking by an electron beam. Second, thin wires were found to have accumulated inside the structure, as highlighted by the red square in Fig. 9a. These wires can also affect beam-wave interaction. They can be removed using ultrasonic methods or a micromanipulator. Finally, the actual size deviates from the design size by 5 μm (about 3%) because of the lack of optical precision during the fabrication process. The aforementioned issues can be resolved through advanced processing techniques and equipment. However, the obtained

outcome was satisfactory because of its superior collimation of the metal column, its periodicity, and its bottom smoothness. The LIGA fabrication technology is suitable for such small structures and high frequencies.

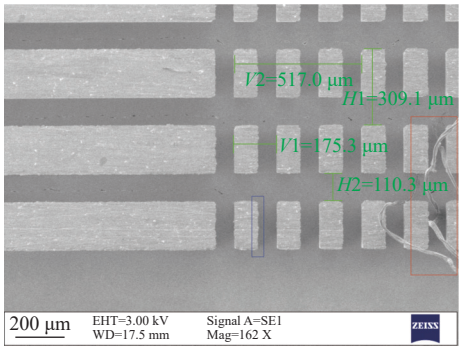

a. Top view of the structure

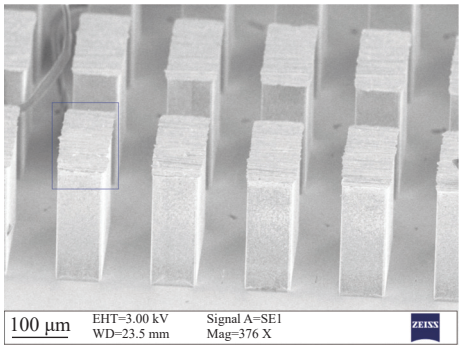

b. Side view of the structure

Fig. 9　High-frequency structure diagram

4　Conclusions

A 0.28-THz BWO, driven by sheet beams, was designed and simulated. The device was based on photonic column array SWS. The SWS allowed beams move through its structure, which effectively reduced the operating current density of the BWO. The simulation results showed that the starting current density was below 6 A/cm^2. The SWS was fabricated using the LIGA fabrication technology. The fabricated structure was satisfactory, and more experimental results will be published in future. This study shows that multi-column SWS represents a viable means for improving the performance of millimeter wave and THz VEDs.

References

[1] TONOUCHI M. Cutting-Edge terahertz technology[J]. Nature Photonics, 2007, 1(2): 97-105.

[2] APPLEBY R, ANDERTON R N. Millimeter-wave and submillimeter-wave imaging for security and surveillance[J]. Proceedings of the IEEE, 2007, 95(8): 1683-1690.

[3] SIEGEL P H. Terahertz technology[J]. IEEE Transactions on Microwave Theory and Techniques, 2002, 50(3): 910-928.

[4] NANNI E A, JAWLA S K, SHAPIRO M A, et al. Low-loss transmission lines for high-power terahertz radiation[J]. Journal of Infrared, Millimeter, and Terahertz Waves, 2012, 33(7): 695-714.

[5] GAO X, YANG Z Q, CAO W P, et al. Dispersion characteristics of a slow wave structure with a modified photonic band gap[J]. Chinese Physics B, 2011, 20(3): 030703.

[6] BRATMAN V L, DUMESH B S, FEDOTOV A E, et al. Terahertz orotrons and oromultipliers[J]. IEEE Transactions on Plasma Science, 2010, 38(6): 1466-1471.

[7] LIU W X, YANG Z Q, LIANG Z, et al. Enhancements of terahertz radiation from a grating waveguide by two-stream instability[J]. IEEE Transactions on Plasma Science, 2008, 36(3): 748-756.

[8] LI R J, RUAN C J, LI S S, et. al. G-band rectangular beam extended interaction klystron based on bi-periodic structure[J]. IEEE Transactions on Terahertz Science and Technology, 2019, 9(5): 498-504.

[9] BAIG A, GAMZINA D, BARCHFEID R, et al. 0.22 THz wideband sheet electron beam traveling-wave tube amplifier: Cold test measurements and beam wave interaction analysis[J]. Physics of Plasmas, 2012, 19(9): 093110.

[10] SHIN Y M, WANG J X, BARNETT L R, et al. Particle-in-Cell simulation analysis of a multicavity W-band sheet beam klystron[J]. IEEE Transactions on Electron Devices, 2011, 58(1): 521-258.

[11] SHIN Y M, BARNETT L R, LUHMANN N C. Quasi-Optical output-cavity design for a 50-kW multicavity W-band sheet-beam klystron[J]. IEEE Transactions on Electron Devices, 2009, 56(12): 3196-3202.

[12] YANG F X, ZHANG X P. A high-efficiency V-band radial-line backward wave oscillator with unilateral slow wave structures[J]. AIP Advances, 2018, 8(10): 105121.

[13] HUNG C L, HONG J H. Stability analysis of a second harmonic coaxial-waveguide gyrotron backward-wave

oscillator[J]. Journal of Infrared Millimeter and Terahertz Waves, 2012, 33(12): 1190-1202.

[14] GAO Y C, CHARLES J R, YU G F, et al. Design and measurement of a sigital phase locked BWO for accurately extracting the quality factors in a biconcave resonator system[J]. Journal of Infrared Millimeter and Terahertz Waves, 2012, 33(3): 357-365.

[15] YANG F X, ZHAN X P. A frequency-tunable V-band radial relativistic backward-wave oscillator[J]. IEEE Transactions on Plasma Science, 2019, 47(5): 2562-2566.

[16] CHEN Q Y, YUAN X S, COLE M T, et al. Theoretical study of a 0.22 THz backward wave oscillator based on a dual-gridded, carbon-nanotube cold cathode[J]. Applied Sciences-Basel, 2018, 8(12): 2462.

[17] TANG X P, YANG Z Q, KHAN K, et al. Theoretical and cold-test investigation of a four-port high-frequency system for a 0.14-THz dual-sheet-beam backward-wave oscillator[J]. IEEE Transactions on Electron Devices, 2018, 65(11): 5068-5074.

[18] KUMAR M, ADITYA S, WANG S M. A W-band backward-wave oscillator based on planar helix slow wave structure[J]. IEEE Transactions on Electron Devices, 2018, 65(11): 5097-5102.

编 辑 叶 芳